

# Fast H-vacancy Dynamics during Alanate Decomposition by Anelastic Spectroscopy. Proposition of a Model for Ti-enhanced Hydrogen Transport

Oriele Palumbo,<sup>†,‡</sup> Annalisa Paolone,<sup>†,§</sup> Rosario Cantelli,<sup>\*,†</sup> Craig M. Jensen,<sup>⊥</sup> and Martin Sulic<sup>⊥</sup>

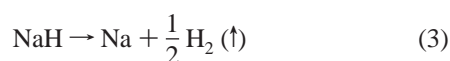
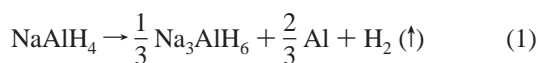
Dipartimento di Fisica, Università di Roma "La Sapienza", Piazzale A. Moro 2, I-00185 Roma, Italy, CNR-INFM Unità di Roma 1, Piazzale A. Moro 2, I-00185 Roma, Italy, CNR-INFM, Laboratorio Regionale SuperMAT, Salerno, Italy, and Department of Chemistry, University of Hawaii, Honolulu, Hawaii 96822

Received: January 19, 2006; In Final Form: March 9, 2006

A systematic study of the dehydrogenation process of undoped and of catalyzed NaAlH<sub>4</sub> by means of anelastic spectroscopy is presented. Evidence is reported of the formation of a highly mobile species during decomposition, which has been identified in off-stoichiometric AlH<sub>6-x</sub> units, giving rise to fast H vacancy local dynamics. The formation of such stoichiometry defects starts at temperatures much lower in Ti doped than in undoped samples, and concomitantly with the decomposition reaction. The catalyst atoms decrease the energy barrier to be overcome by H to break the bond, thus enhancing the kinetics of the chemical reactions and decreasing the temperature at which the dehydrogenation processes take place. The experimental data show that not all the hydrogen released by the formula units during the evolution of decomposition evolves out of the sample, but part of it remains in the lattice and migrates on a long-range scale within the sample. We identify, in this H mobilized population, the species which induces the fast tetragonal to monoclinic phase transformation accompanying decomposition. A partial spontaneous thermally activated regression of decomposition has also been observed by aging experiments. A model is proposed which accounts for the action of the Ti catalyst and for the atomistic mechanism of decomposition.

## Introduction

Sodium alanate, NaAlH<sub>4</sub>, is considered among the most promising compounds for solid-state hydrogen storage. The hydrogen release from these materials occurs by means of three chemical reactions that take place at increasing temperatures:



The thermodynamics of the first two reactions are compatible with onboard vehicular hydrogen storage applications, whereas the last reaction occurs at a temperature too high to be of practical interest. The addition of a catalyst, such as Ti or Zr makes reactions 1 and 2 reversible, reduces the decomposition temperatures, and enhances the kinetics of dehydrogenation and re-hydrogenation of the compound to rates that are of practical relevance.<sup>1</sup> Despite large efforts, the atomistic paths during the tetrahydride–hexahydride decomposition reaction, and the mechanism of action of the catalyst are still unknown. The position of the catalytically active species in the lattice

(substitutional or interstitial) and the exact nature and role of the Al–Ti alloys that are formed on repeated hydrogen cycling of the material is a matter of intense debate.<sup>2–8</sup> Various authors<sup>9–11</sup> invoked the existence of a highly mobile entity in order to explain the transitions (1) and (2). However, no experimental data or decisive information has been reported to date that directly reflects the various steps of decomposition and the mechanism of action of the catalyst.

Recently, it was observed by anelastic spectroscopy measurements<sup>12</sup> that heating of sodium alanates to temperatures at which decomposition occurs causes the formation of a highly mobile point defect complex, as detected by the appearance of a thermally activated relaxation process at low temperature (~70 K for a vibration frequency of 1 kHz). It was also shown that the onset and evolution of the chemical reactions in the alanates can be monitored by the variations of their elastic moduli. It was suggested<sup>12</sup> that the discovered relaxing species should involve hydrogen, and the following possible mechanisms for the relaxation peak were proposed: (i) the relaxation of H in the NaH compound produced by the decomposition reaction 2; (ii) the reorientation of H around Ti, or Ti–Al complexes; (iii) a stoichiometry defect of Na<sub>3</sub>AlH<sub>6</sub> (such as a H vacancy).

In the present paper we report a systematic study of the dehydrogenation of undoped and Ti-doped NaAlH<sub>4</sub>. The observation of the deuterium-isotope peak shift suggests that the mobile species causing the relaxation process is a point defect complex involving hydrogen. The peak is observed in both the catalyzed and the undoped samples, thus excluding that this process requires the presence of Ti. However, the number of the relaxing species formed on thermally cycling is much higher in the catalyzed samples. Our experimental evidence supports the hypothesis that the peak is caused by the

\* Corresponding author phone: +39-06-49914388; fax: +39-06-4957697; e-mail: Rosario.Cantelli@roma1.infn.it.

<sup>†</sup> Dipartimento di Fisica, Università di Roma.

<sup>‡</sup> CNR-INFM Unità di Roma 1.

<sup>§</sup> Laboratorio Regionale SuperMAT.

<sup>⊥</sup> University of Hawaii.

relaxation of hydrogen vacancies in off-stoichiometry groups of type  $\text{Na}_3\text{AlH}_{6-x}$ . It is proposed that the drop of the decomposition temperatures and the kinetic acceleration in catalyzed samples are due to the lowering of the energy necessary to break the Al–H bonds of the  $\text{AlH}_6$  complex anions induced by the addition of Ti. Furthermore, evidence is produced that the hydrogen released by the formula units at the decomposition temperatures diffuses within the lattice with remarkable mobility.

## Experimental Section

Sodium aluminum hydride was obtained from Albemarle Corp. The aluminum metal was removed from the raw hydride via Soxhlet extraction with dry, oxygen-free tetrahydrofuran (THF) under a nitrogen atmosphere using the standard Schlenk technique. The final purification was accomplished through recrystallization from THF/pentane.  $\text{NaAlD}_4$  was synthesized from  $\text{LiAlD}_4$  (Aldrich, 99.8% isotopic purity) and NaF as described in the literature.<sup>13</sup> Sodium aluminum hexahydride  $\text{Na}_3\text{AlH}_6$  was synthesized and purified by the method of Huot et al.<sup>14</sup> Doping of all the powders was performed by the mechanical milling method<sup>15–17</sup> in which the hydride (deuteride) was combined with 2 mol %  $\text{TiF}_3$  (Aldrich, purity 99%) and ball-milled under an argon atmosphere in a stainless steel bowl using a Fritsch 6 planetary mill at 400 rpm and a grinding ball-to-powder ratio of 35:1.

To perform anelastic spectroscopy measurements consolidated vibrating samples are needed. Alanates are available as powders which cannot be sintered at high temperature. Therefore, two different procedures were followed to obtain self-sustained samples. In the case of  $\text{NaAlH}_4$  samples doped with 2%  $\text{TiF}_3$  and labeled as Ti2%H-2 and Ti2%H-5,  $\text{Na}_3\text{AlH}_6$  doped with 2%  $\text{TiF}_3$  (sample Ti2%H-1hexa) and the deuterated specimen doped with 2%  $\text{TiF}_3$  (sample Ti2%D-1), the alanate was mixed with pure KBr powder, which acts as a compactant, and then pressed. For the Ti doped samples Ti2%H-6 and Ti2%H-8 and two undoped  $\text{NaAlH}_4$  samples (UH-1 and UH-2), alanate powder was pressed and equally compacted samples were obtained without the use KBr. All samples were bars 40 mm long, 5 mm wide and 0.7–1.5 mm thick. Some bars made of pure KBr were also prepared for reference. As the alanate powder reacts with oxygen and water vapor, all operations were accomplished in a glovebag in flowing nitrogen atmosphere.

Anelastic spectroscopy measurements are conducted suspending the bars on thin wires located at the nodal lines of flexural vibration modes, and electrostatically exciting the corresponding mechanical resonances of the samples; in the present work, the first and third flexural modes were excited. The sample vibration produces an alternate stress which interacts with the local lattice distortions introduced by the mobile entities and perturbs their site energies in such a way that the sites that are energetically favored in the first half period become unfavored in the second half. The system then looks for the equilibrium redistribution among the perturbed levels. At the temperature at which the relaxation rate  $\tau^{-1}$  of the species is equal to the angular vibration frequency  $\omega$  ( $\omega\tau = 1$ ), the stimulated atomic migration is able to follow, by thermal activation, the sample vibration, and the coefficient of elastic energy dissipation  $Q^{-1}$  reaches its maximum value. The energy dissipation (or reciprocal of the mechanical quality factor  $Q$ ) is measured from the decay of the free oscillations or from the width of the resonance peak. The measurement of the dynamic Young modulus  $E'$  is simultaneously obtained from the angular vibration frequency  $\omega^2 = kE'/\rho$ , where  $\rho$  is the mass density and  $k$  is a numerical factor

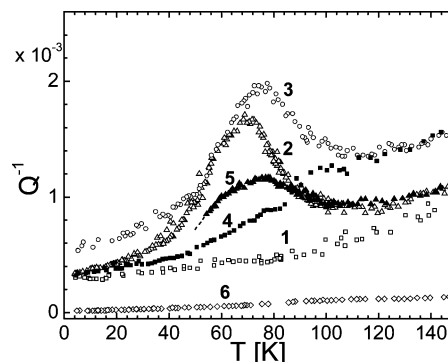


**Figure 1.** Low-temperature dependence of the elastic energy loss of sample Ti2%H-2 as prepared ( $\square$ , 1) and after a thermal treatment at 436 K ( $\Delta$ , 2, 1.1 kHz;  $\circ$ , 3, 4.8 kHz); sample Ti2%D-1 as prepared ( $\blacksquare$ , 4) and after a thermal treatment at 441 K ( $\blacktriangle$ , 5, 1.1 kHz); KBr sample as prepared ( $\diamond$ , 6).

depending on the sample geometry.<sup>18</sup> The independent and concomitant measurements of  $Q^{-1}$  and  $E'$  allow the complex modulus  $E = E' + iE''$  to be derived, being  $Q^{-1} = E''/E'$ . For a single relaxation time,  $\tau$ ,  $Q^{-1}$  is given by the following:

$$Q^{-1} = g\nu_0(\lambda_1 - \lambda_2)^2 \frac{cn_1n_2}{kT} E' \frac{(\omega\tau)^\alpha}{1 + (\omega\tau)^{2\alpha}} \quad (4)$$

where  $c$  is the molar concentration of the jumping atoms and  $n_1$  and  $n_2$  their equilibrium fractions in sites 1 and 2;  $\lambda_1$  and  $\lambda_2$  are the elastic dipoles<sup>18</sup> of the defects in the two configurations;  $g$  is a factor of the order of  $1/2$  depending on the geometry of the jump and the type of sample vibration,  $\nu_0$  the unit cell volume,  $\alpha$  a parameter equal to 1 for a single-time Debye process, and  $k$  the Boltzmann constant. For classical processes is  $\tau = \tau_0 e^{W/kT}$ , being  $W$  the activation energy. As  $\tau$  is temperature-dependent for thermally activated processes, the relaxation condition ( $\omega\tau = 1$ ) is satisfied at low temperatures for fast processes and at high temperatures for slow processes.

## Results

**Isotope Effect.** To ascertain whether the mobile species giving rise to the anelastic peak involves hydrogen, we performed measurements on both hydrogenated and deuterated samples. Figure 1 shows a comparison between the low-temperature spectra of  $\text{NaAlH}_4$  (Ti2%H-2) and  $\text{NaAlD}_4$  (Ti2%D-1) doped with 2%  $\text{TiF}_3$ . Both samples were obtained by mixing the alanate powders with KBr and pressing. In the as-prepared state, the samples show a monotonically increasing background with an increase of temperature. For reference, the dissipation of a sample produced by pressing only the KBr powder was measured, and, as seen in Figure 1, it consists of a very low background. After heating sample Ti2%H-2 to 436 K as previously described,<sup>12</sup> a well-developed peak appeared. This process is thermally activated as it shifts toward a higher temperature at the higher vibration mode (Figure 1). The activation energy for the relaxation process obtained from the hydrogen containing sample is 0.126 eV and the preexponential factor is  $7 \cdot 10^{-14} \text{ s}^{12}$  which is typical of point defect relaxation. The peak is very broad with respect to a single Debye process, indicating strong elastic interactions and/or multiple jumping type of the mobile entity. Indeed, the peak can be fitted<sup>12</sup> considering a Gaussian distribution for both the activation energy and the relaxation time; the best fit values of the standard deviation of the distribution are  $\sigma(E) = 0.022 \text{ eV}$  and  $\sigma(\tau_0) = 3 \times 10^{-15} \text{ s}$ .

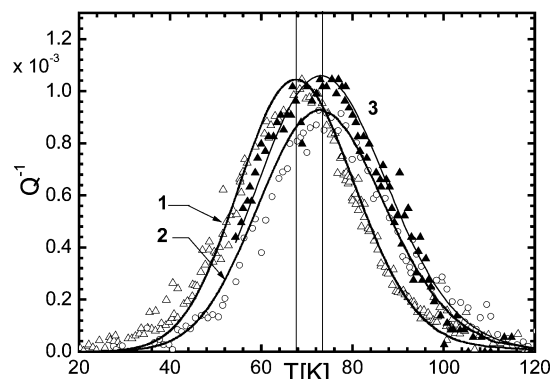


**Figure 2.** Elastic energy loss of sample Ti2%H-2 after a thermal treatment at 436 K ( $\Delta$ , 1, 1.1 kHz;  $\circ$ , 2, 4.8 kHz); sample Ti2%D-1 after a thermal treatment at 441 K ( $\blacktriangle$ , 3, 1.1 kHz). A linear background has been subtracted from the measurements reported in Figure 1. The heights of the two peaks measured at 1.1 kHz have been normalized. Lines are the best fit considering a Gaussian distribution for both the activation energy and the relaxation time. The vertical lines mark the position of the maxima of the peaks in the hydrogenated and deuterated samples.

The NaAlD<sub>4</sub> sample doped with Ti was thermally treated from the as-prepared state with subsequent cycles up to 323, 345, 368, and 441 K. Only after the last treatment (441 K for 100 minutes) did sample Ti2%D-1 exhibited the peak seen in Figure 1. The higher temperature and longer time of the treatment necessary to introduce the peak indicate that the decomposition and outgassing kinetics of the deuterium-containing samples is shifted to a higher temperature with respect to hydrogen. It is also noticed that the peak in the deuterated sample is shifted to a higher temperature by  $\sim 7$  K with respect to that of the hydrogenated specimen (measured at about the same frequency, 1.1 kHz). This shift is well above the experimental uncertainty of the temperature measurement, which is 0.1 K. In addition, the difference of about 30 K of the vibration frequency of the two samples at the peak temperature cannot account for the shift. To obtain a quantitative analysis of the peak in the deuterium-containing sample we fitted the experimental data, after subtraction of a linear background, considering a Gaussian distribution for both the activation energy and the relaxation time, similarly to the case of NaAlH<sub>4</sub>. The best fit values of the mean and of the standard deviation of the energy distribution are  $\bar{E}_D = 0.136$  eV and  $\sigma(E_D) = 0.025$  eV, compared with  $\bar{E}_H = 0.126$  eV and  $\sigma(E_H) = 0.022$  eV, obtained for hydrogen. For the mean and the standard deviation of the relaxation time distribution we fixed the values obtained from the hydrogenated sample (Figure 2).

The isotope shift of the peak suggests that the relaxation at low temperature is caused by the dynamics of a complex containing hydrogen. As H is known to show fast dynamic in solids, this fact should not be unexpected.

**Ti Doped NaAlH<sub>4</sub>.** To obtain more information about the nature of the relaxing complex, a systematic study of the anelastic spectrum during the thermally activated reactions has been conducted.

**High-Temperature Measurements.** Figure 3 reports the high temperature  $f$  curves for samples Ti2%H-6 and Ti2%H-8, obtained by pressing the NaAlH<sub>4</sub> powder doped with 2% TiF<sub>3</sub>, without addition of KBr. During the thermal cyclings up to 360 K the  $f$  curves show hysteresis loops which close on cooling back to room temperature, indicating practically no onset of the chemical reactions. Instead, the cycles extended to higher temperatures remain open and, principally, the elastic modulus

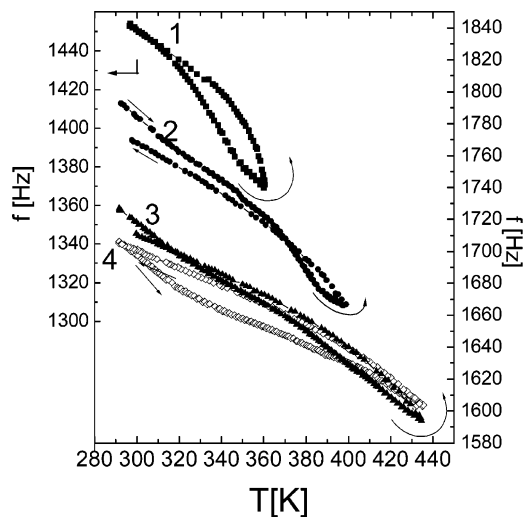


**Figure 3.** Temperature dependence of the frequency of sample Ti2%H-6 during a thermal cycle up to 360 K ( $\blacksquare$ , 1); sample Ti2%H-8 during a thermal cycle up to 400 K ( $\bullet$ , 2) and a cycle up to 435 K ( $\blacktriangle$ , 3), and a subsequent cycle up to 436 K ( $\diamond$ , 4).

markedly decreases from cycle to cycle (see curves 1, 2, and 3 in Figure 3). The former feature and the visible softening indicate a substantial change of the nature of the material. This change is explained by the progressive formation of a new phase during decomposition, which is accompanied by the hydrogen evolution out of the sample according to eqs 1 and 2. A thermal cycle to a temperature previously reached (curve 4 of Figure 3) or to a lower one causes only a little further modulus variation, and this indicates substantial arrest in the progression of the decomposition reactions. But a successive cycle to a higher temperature, again, keeps producing further softening, i.e., a restarting in the progression of decomposition. The samples compacted with KBr displayed results congruent with those of pure alanate, in particular, the softening of the material after each thermal cycle above 360 K.

Also the enhancement of the porosity we observed on the samples may play a secondary role in the measured softening; it is well-known that the apparent Young's modulus (and, therefore, the vibration frequency) decreases when porosity increases. However, we did not observe a visible porosity increase after thermal cycles up to a temperature lower than that previously reached, during which there is only little further modulus variation and no progression of decomposition. Therefore, the enhancement of porosity is the signature of the progression of the chemical reactions.

**Low-Temperature Measurements.** Each high-temperature treatment, and the concomitant  $f$  and  $Q^{-1}$  measurements, was followed by a low-temperature run. Figure 4 shows the low-temperature dissipation curves of the NaAlH<sub>4</sub> samples Ti2%H-6 and Ti2%H-8 doped with 2% TiF<sub>3</sub> after the respective thermal aging reported in Figure 3. The sample that previously displayed a closed loop when heated to 360 K (curve 1 in Figure 3) showed a smooth background dissipation on cooling. After the TT to 380 K, a peak appears at  $\sim 70$  K with a vibration frequency of 1 kHz (curve 2 in Figure 4), which develops in height after subsequent thermal treatments to progressively higher temperatures. Most notably, the peak grows after heating the sample to 400 K, during which the elastic modulus indicated that decomposition proceeded (curve 2 in Figure 3), but remains unchanged after a subsequent TT at a temperature of 20 K lower (380 K, curve 4 in Figure 4) than the previous one during which decomposition did not proceed substantially. After increasing



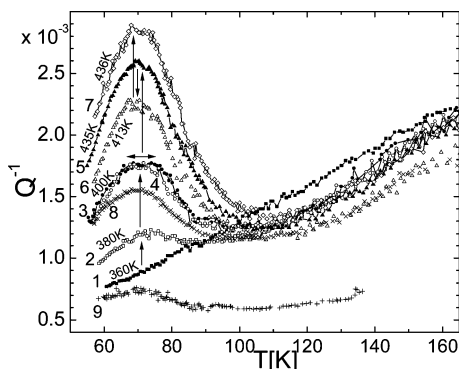


**Figure 4.** Low-temperature dependence of the elastic energy loss. Sample Ti2%*H*-6 after a thermal treatment (TT) up to 360 K (■, 1). Sample Ti2%*H*-8 after the following subsequent TT's up to: 380 K (□, 2); 400 K (●, 3); 380 K (○, 4); 435 K (▲, 5); 413 K (△, 6); 436 K (◇, 7). Sample Ti2%*H*-5 (mixed with KBr) after TT up to 436 K (x, 8). Sample UH-2 after two subsequent TT at 441 K of 240 min each as described in Figure 5 (+, 9).

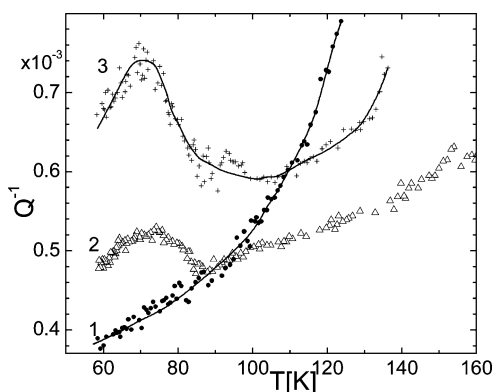


**Figure 5.** Low-temperature dependence of the elastic energy dissipation of: the undoped sample: UH-1 as prepared (●, 1); sample UH-2 after a first thermal treatment of 240 min at 447 K (△, 2) and after a second thermal treatment of further 240 minutes at 447 K (+, 3). Lines are guides to the eyes.

the TT to 435 K, the peak height increase proceeds (curve 5 in Figure 4). Instead, a subsequent TT at a lower temperature (413 K) visibly reduces the peak height. This is an important result which indicates regression of the concentration of the mobile species produced by decomposition, i.e., partial spontaneous thermally assisted reversion of the decomposition reaction. After a further increase of the high-temperature aging, the peak height keeps intensifying again. These results link the appearance and the evolution of the height of the peak at low temperature to the softening of the elastic modulus at high temperature, and indicate that both features constitute a powerful tool to monitor the onset and the progression of the decomposition reaction in alanes. As a reference, the low-temperature peak, obtained in samples mixed with KBr,<sup>12</sup> is also shown in Figure 4 (curve 8). The comparison between the dissipation curves of the pure and mixed alanes confirms previous cross-checking experiments conducted,<sup>12</sup> and let us conclude that potassium bromide behaves simply as a neutral compacting medium and does not alter the structure of the relaxation process.

**Undoped NaAlH<sub>4</sub>.** The series of thermal treatments and the subsequent measurements below room temperature were also repeated in pure undoped NaAlH<sub>4</sub>, and the results are shown in Figure 5. Even after the thermal treatment at 436 K (i.e., close to melting), which was the temperature at which an intense peak was stimulated in the Ti containing samples (Figure 4), the low-

temperature peak did not appear. This means that no decomposition reaction started at this temperature, as already known from X-ray diffraction data,<sup>11</sup> that reported a shift of the onset of the decomposition of 50–70 K to higher temperature in undoped samples. Eventually, a thermal treatment at 447 K for 240 min introduced a small peak centered at 70 K with features identical to those found in the catalyzed samples. To enhance the peak, and due to the impossibility of increasing the annealing temperature without reaching the melting temperature ( $T_M = 456$  K),<sup>19</sup> an aging was carried out for a second time at the same temperature of 447 K for 240 min to allow the reaction to proceed. The measurement of elastic energy dissipation below room temperature after the second TT at 447 K yielded an increase of the peak height by a factor of 2, as shown in Figure 5. Indeed, in situ X-ray diffraction measurements revealed a partial conversion of tetrahydride into hexahydride<sup>11</sup> by keeping the sample at 447 K for 300 min and, on further aging at the same temperature, the onset of the high-temperature decomposition reaction was also observed with the formation of a small amount of NaH.

It is important to note that, despite the long-lasting high-temperature annealings of the undoped samples, the peak heights are negligible (curve 9 of Figure 4) with respect to those displayed by the Ti-containing samples, and in particular to the sample treated at an even lower temperature (curve 7 of Figure 4). This means that the reactions in the undoped samples, even though they are heated close to the melting temperature, proceeded at very low rates.

## Discussion

**Possible Sources of the Fast Dynamic Process.** The low temperature peak presently studied is not due to the tetrahydride phase, as it is absent in the initial NaAlH<sub>4</sub> compound before decomposition. The relaxation of hydrogen connected with one of the stoichiometric products of decomposition, Na<sub>3</sub>AlH<sub>6</sub>, Ti–Al clusters, segregated metallic Al, and NaH, is excluded, too. In fact: (a) elastic energy dissipation measurements in the Na<sub>3</sub>AlH<sub>6</sub> hexahydride sample Ti2%*H*-1hexa in the as-prepared state did not show the low temperature peak and, indeed, hydrogen relaxation in a stoichiometric compound would hardly be expected due to the absence of free sites for H reorientation; (b) the reorientation of H around Ti or a Ti–Al complex cannot be considered, as the peak appears also in the undoped (Ti-free) alanate (Figure 5); (c) hydrogen in metallic Al cannot account for the peak, as the solubility of H in bulk Al is such low ( $H/Al = 10^{-6}$ – $10^{-8}$  at 660 °C) that the intense peak observed cannot be thought to be produced by defects present at ppm fractions (see eq 4);<sup>20</sup> (d) the possibility of H relaxation in the NaH compound produced by the decomposition reaction 2 is quite unlikely as the peak is detected already after a TT at 380 K, i.e., at the onset of the first decomposition reaction, whereas NaH formation takes place at higher temperature during the third reaction. Also XRD measurements<sup>11</sup> exclude the presence of a significant amount of NaH after aging at 380 K for a short time. In addition, our recent  $Q^{-1}$  measurements on NaH did not reveal any dissipation process below room temperature.

In view of the above considerations, the formation of an off-stoichiometric unit must be invoked during the decomposition process producing the tetrahydride–hexahydride phase transformation to account for the mechanism of the peak at 70 K. The most likely off-stoichiometric unit is a defect hexahydride of type Na<sub>3</sub>AlH<sub>6-x</sub> in which one or more H atoms are missing in the formula unit. This group would possess one or more H

vacant sites which would allow the remaining H atoms to reorient around Al. Such a structure would give rise to a vacancy dynamics mechanism thoroughly compatible with the low-temperature peak observed.

#### Proposition of an Atomistic Mechanism of Decomposition.

To explain the experimental data previously reported, we propose the following model for the atomistic mechanism of the dehydrogenation reactions, taking into account the high mobility of hydrogen.

The decomposition reaction starts at temperatures at which hydrogen has sufficient thermal energy to break the covalent Al–H bond of  $\text{NaAlH}_4$  ( $T > 360$  K, curve 1 in Figure 3). After dissociation, the H atoms interstitially migrate within the lattice of initial tetragonal symmetry. Via diffusion-controlled hopping, they visit the  $\text{AlH}_4$  units and rearrange themselves around a tetrahydride structure to transform it into a hexahydride symmetry by the involvement of two additional Na atoms located in the neighboring tetrahydride units. Part of the hydrogen made free migrates to the surface and evolves as gas out of the sample after recombination in molecular form. In the H rearrangement, off-stoichiometric groups are produced consisting of  $\text{AlH}_{6-x}$  units resulting from imperfect recombination, all of which being missing one or more H atoms. Indeed, it has been proved that the hydrogen insertion in interstitial occupancy in metals is energetically favored in combination with host atoms vacancies.<sup>21</sup> If one or more of the 6 H atoms are missing in the  $\text{Na}_3\text{-AlH}_6$  formula unit, jumping around Al is possible for the remaining H atoms, or in other words, H vacancy dynamics may take place. When this occurs, a multi-well potential with nearly equal energy minima is formed around the Al which is coordinated with the vacancy hopping. The marked broadness of the peak may say that it is not caused by a single process as more than one type of  $\text{AlH}_{6-x}$  complex (with different  $x$  and  $\tau^{-1}$ ) contributes to relaxation, or that it may be caused by the interaction among complexes or by multiple H occupancy.<sup>18</sup>

The Al atoms resulting in excess during the tetra–hexa transformation remain dispersed and slowly cluster in form of crystals in the lattice.<sup>2–8</sup> Only after a few H charge/discharge cycles Al–Ti islands begin to be observed,<sup>2–8</sup> as the associated thermal treatments allow migration and agglomeration of the heavy Al and/or Ti atoms. The repeated cycles required before the appearance of the Al–Ti islands show that metal diffusion is slow in alanates and, in particular, remarkably slower than the hydrogen interstitial motion. In this framework, the structural transformation can be considered as driven by hydrogen dynamics, rather than by Al or Al–H complexes motion.

During the subsequent thermal treatments to progressively higher temperatures shown in Figure 3, the height of the decomposition peak increases (Figure 4) as the concentration of  $\text{AlH}_{6-x}$  units increases with the progression of decomposition. Concomitantly, interstitial atomic hydrogen is released by the reaction into the lattice under nonequilibrium conditions and is partly desorbed. Instead, when an annealing of the sample is made at a temperature lower than that of the previous TT, very little softening of the elastic modulus is observed (curve 4 of Figure 3), indicating that no significant decomposition took place. Correspondingly, the low temperature measurement following this treatment displays a decrease of the peak height, as shown by curve 6 of Figure 4. It means that the hydrogen population, previously injected in the lattice under nonequilibrium conditions, looking for equilibrium, partially migrated back to the bond sites, which evidently provide deeper site energies for H, thus reducing the concentration of the  $\text{AlH}_{6-x}$  relaxing defect units responsible for the process.

The fact that the TT at 380 K after the annealing at 400 K left the peak height unchanged (curve 4 of Figure 4) can be understood to result from H having insufficient thermal activation to perform the redistribution migration.

The observation of the decrease of the peak height under the conditions illustrated above (Figure 4, curve 6) is of relevant importance as it demonstrates the following: (a) not all the hydrogen released by the decomposition evolves out of the sample as gas but partly remains in the lattice, and slightly above 400 K is able to migrate on a long-range scale to change the concentration of the relaxing units; (b) a partial spontaneous reverse transformation can take place in alanates, with no need of pumping-in hydrogen at high pressure. This occurs as a result of the presence of the hydrogen stored in the reservoir constituted by the crystal lattice, which feeds the reverse transformation.

The result that the H population is visibly mobile on a long-range scale in the crystal lattice starting from about 400 K allows a more complete picture of the hydrogen dynamics in alanates over the whole temperature range to be attained. Precisely, above about 400 K, hydrogen performs about  $10^{11}$  local jumps per second around Al, but also has the thermal activation to diffuse through the lattice. It means that a small fraction of the fast local jumps results in H dissociating from the  $\text{AlH}_{6-x}$  group, migrating to neighboring groups by a hopping process, and fast relaxing around them before diffusing again. Below those temperatures, and in particular at the temperatures at which the reorientation process appears at the acoustic frequencies (70 K), H can reorient around Al due to the low activation energy for relaxation measured ( $E_R = 0.126$  eV) with a rate of the order of  $10^3$  s<sup>-1</sup>, but it has not the thermal activation to leave the bond.

**Role of the Ti Catalyst.** The local dynamics of H vacancies gives rise to the dissipation peak at low temperature; the experiments themselves are evidence that the activation energy for this process is the same in undoped and catalyzed samples. However, after thermally cycling both compounds at the same temperature, the intensity of the peak, and therefore, the concentration  $c_H$  of H vacancies is much higher in the Ti-containing samples than in the undoped specimen. The content  $c_H$  depends on the energy barrier that H must overcome to break the Al–H bond: the higher the barrier, the lower  $c_H$ . Considering the experimental results shown above, we propose the potential energy profile of a H atom in the undoped and in the catalyzed alanate depicted in Figure 6. Let us call  $E_C$  and  $E'_C$  (Figure 6a) the heights of the potential barriers that H must overcome in the undoped compound to break the stoichiometric Al–H chemical bond in the  $\text{AlH}_6$  and in the imperfect units  $\text{AlH}_{6-x}$ , respectively.  $E'_C$  was chosen to be smaller than  $E_C$  as the site energy of an H atom in the defect unit, and it is expected to be higher than that in the filled complex.  $E_R = 0.126$  eV<sup>12</sup> is the activation energy for the H-vacancy reorientation in the  $\text{AlH}_{6-x}$  group which gives rise to the peak observed at 70 K.  $E_I$  is the height of the potential energy barrier for the interstitial long-range H migration in the lattice.

The decrease of about 100 K of the onset of the reactions and the much higher  $c_H$  in the catalyzed samples with respect to the undoped ones means that Ti decreases the heights of the potential barriers that H must overcome for bond dissociation, labeled  $E''_C$  and  $E'''_C$ . This activation energy decrease may result from an increase of the H site energy in the bond and/or from a lowering of its saddle point energy. We note that, according to the Boltzmann statistics, even a small decrease of the barrier of 0.1 eV produces an increase of the H dissociation probability

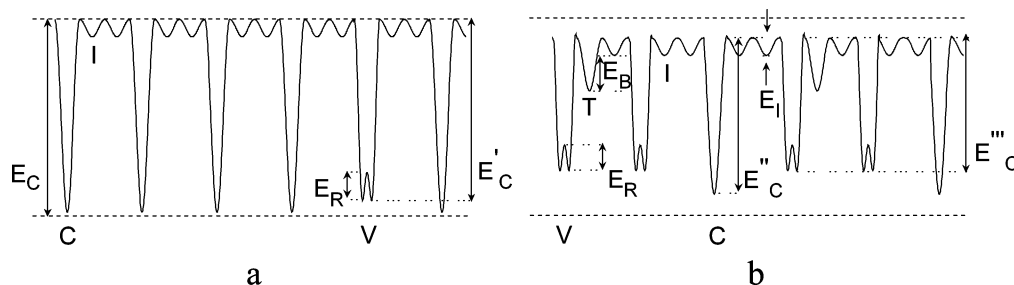


**Figure 6.** Schematic representation of the proposed potential energy of H atoms in thermally treated NaAlH<sub>4</sub>: (a) undoped and (b) Ti-doped. Minima correspond to chemical bond sites (labeled as C), lattice sites coordinated with the titanium trap (T), interstitial sites (I), and vacancy sites (V).  $E_R = 0.126$  eV<sup>12</sup> is the activation energy for vacancy relaxation (reorientation) and  $E_C$ ,  $E'_C$ ,  $E''_C$  and  $E'''_C$  are the energies for H to break the bonds.  $E_I$  is the activation energy for H interstitial migration,  $E_B$  the binding energy of H to Ti.

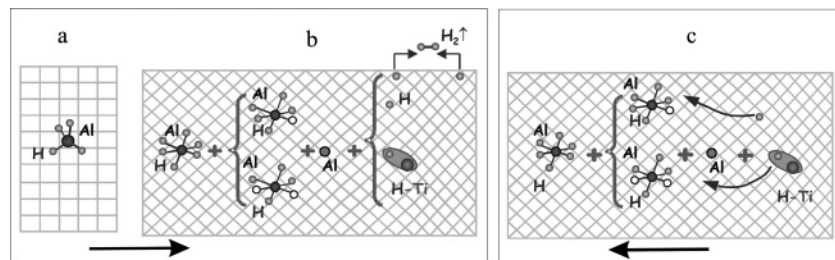


**Figure 7.** Schematic representation of the proposed dehydrogenation model: (a) AlH<sub>4</sub> group of initial NaAlH<sub>4</sub>; (b) products of thermal decomposition: formation of both AlH<sub>6</sub> and AlH<sub>6-x</sub> units, segregated Al, interstitial H in free and Ti trapping sites. The H atoms migrating to the surface recombine as a molecules and evolve as gas. (c) reverse H migration to the deepest trap (chemical bond) during a subsequent thermal treatment in which the decomposition reaction does not proceed significantly, and allows partial equilibrium to be reached.

of a factor of 10. The activation energy  $E_R$  for the local H vacancy dynamics in AlH<sub>6-x</sub> has been assumed to be the same in the undoped and Ti-doped compounds, as the low-temperature decomposition peak appears at the same temperature in the two cases (Figures 4 and 5).

Transmission electron microscope observations revealed that, in NaAlH<sub>4</sub> doped with 2 mol % TiF<sub>3</sub>, the Ti is initially distributed as TiF<sub>3</sub> crystallites and, in a minor proportion, as dispersed Ti atoms incorporated into the alanate phase.<sup>6</sup> Despite the low concentration of Ti dispersed in the alanate, the Ti-modified potential profile can be extended over the whole sample, as reported in Figure 6b, because the elastic interactions are effective on a long-range scale. It is important to note that the present model would be valid regardless of the Ti location in the material.

The action of Ti is not expected to be limited only to the energies of the H bond sites, as discussed above, but also to those of the nearest and next nearest interstitial lattice sites to Ti. This action very likely consists of Ti behaving as a trapping center for interstitial H. The trapping of H by substitutional impurities was first reported for Nb–Ti–H dilute alloys in 1977,<sup>22,23</sup> and recently reviewed.<sup>24</sup> In Nb, substitutional titanium captures H in the 1:1 atomic ratio, and is the most effective trap found (even compared to Zr<sup>24</sup>), likely due to its great affinity to H. The activation energy for the H long-range migration in Nb ( $E_M = 0.10$  eV) derived from Gorsky effect measurements,<sup>25</sup> is increased to 0.16 eV by the presence of substitutional Ti dissolved in the lattice.<sup>26</sup> As a consequence of such a barrier deepening, the mean stay time of H in the Ti traps is increased so much with respect to that in the free lattice sites, that H hopping essentially proceeds from trapping site to trapping site. This capture hinders the H–H atom interaction and prevents hydride precipitation by keeping H in solid solution around Ti. The role of Ti as a trap for H is corroborated by recent ab initio calculations in sodium alanates,<sup>27</sup> which revealed that substitutional Ti is a powerful hydrogen attractor. Indeed, recent works

of Raman scattering and ab initio calculations<sup>28</sup> in undoped NaAlH<sub>4</sub> suggest that the enhanced absorption and desorption kinetics is due to the effectiveness of Ti in promoting the breakup of the AlH<sub>4</sub> anions (by a weakening of the Al–H bond strength), during the first reaction.

Thus, there are two effective types of traps for H in alanates, the bond and the Ti catalyst. If we call as  $E_B$  the energy deepening (or binding energy) of the interstitial sites coordinated with Ti (labeled as trap sites), according to the present model, a thermally controlled competitive distribution among the interstitial sites, the trap sites, and the bond sites can take place on aging. Which trap is the deepest is definitely indicated by the experiment of curve 6 in Figure 4. In the thermal treatment at 413 K, which did not cause further decomposition, the H population started approaching the equilibrium distribution among the traps. The decrease of the peak height after this treatment indicates reversion of H atoms to the relaxing AlH<sub>6-x</sub> units and hence an enrichment of the bond sites and a consequent depletion of the Ti trap sites. This experiment clearly demonstrates that the chemical bond is the deepest trap.

In Figure 7a schematic summary of the steps and the products of the two-way reactions during the various thermal treatments are presented, according to the present model.

High pressure, in situ synchrotron X-ray diffraction studies of the rehydrogenation of the doped hydride have shown that this process proceeds through the exact microreverse of the dehydrogenation process.<sup>29</sup> Therefore, it can be inferred that rehydrogenation proceeds through the reverse of the process, as depicted in Figure 7c. Thus we have, for the first time, gained a detailed insight into this, heretofore enigmatic, process. Experiments designed to study in detail the reverse transformation are currently underway in our laboratories.

## Conclusions

The formation of a new species and its evolution during the decomposition reactions in Ti-doped and undoped sodium



alanates was observed for the first time by anelastic relaxation spectroscopy. This species, which gives rise to a thermally activated relaxation peak around 70 K at 1 kHz, is very mobile and clearly a point-defect complex, which according to the observed deuterium isotope shift, involves hydrogen. Various possible sources of the process have been considered, taking into account the products of decomposition. After excluding any stoichiometric product of decomposition and even the involvement of catalytic Ti, it is concluded that the most likely cause of the observed process is a hexahydride stoichiometry defect of type  $\text{AlH}_x$  ( $x < 6$ ) missing one or more H atoms, thus giving rise to local vacancy dynamics. The results show that not all the hydrogen released during the high temperature decomposition reactions evolves out of the samples as gas, but part of it remains in the lattice and diffuses on a long-range scale. At high temperature, a spontaneous partial reverse decomposition reaction has been monitored. At low temperature the long-range mobility of H is frozen and only a local dynamics around Al takes place. Our data demonstrate that the  $\text{AlH}_{6-x}$  bond is a deeper trap for H than Ti. A model has been formulated which explains the catalytic effect of Ti and the decomposition mechanism, in which hydrogen is identified as the long-range mobile species inducing the tetragonal–monoclinic phase transformation connected with decomposition.

**Acknowledgment.** This work was supported by the Ministry of Education, University, and Research (MIUR) through a project PRIN 2004, and by the Office of Hydrogen, Fuel Cells and Infrastructure Technologies of the U.S. Department of Energy. We thank T. De Angelis and D. Nicoletti for help in some of the anelastic spectroscopy experiments and A. Iacoangeli for technical assistance.

## References and Notes

- (1) Bogdanovic, B.; Schwickardi, M. *J. Alloys Compd.* **1997**, 253–254, 1.
- (2) Brinks, H. W.; Jensen, C. M.; Srinivasan, S. S.; Hauback, B. C.; Blanchard, D.; and Murphy, K. *J. J. Alloys Comd.* **2004**, 376, 215.
- (3) Felderhoff, M.; Klementiev, K.; Grunet, W.; Spliehoff, B.; Tesche, B.; von Colbe, J. M. B.; Bogdanovic, B.; Hartel, M.; Pommerin, A.; Schuth, F.; Weidenthaler, C. *Phys. Chem Chem. Phys.* **2004**, 6, 4369.
- (4) Leon, A.; Kircher, O.; Rothe, J.; Fichtner, M. *J. Phys. Chem. B* **2004**, 108, 16372.

- (5) Graetz, J.; Reily, J. J.; Johnson, J.; Igatov, A. Y.; Tyson, T. A. *Appl. Phys. Lett.* **2004**, 85, 500.
- (6) Andrei, C. M.; Walmsley, J.; Brinks, H. W.; Holmstad, R.; Jensen, C. M.; Hauback, B. C. *Appl. Phys. A* **2005**, 80, 709.
- (7) Brinks, H. W.; Hauback, B. C.; Srinivasan, S. S.; Jensen, C. M. *J. Phys. Chem. B* **2005**, 109, 15780.
- (8) Kuba, M. T.; Eaton, S. S.; Morales, C.; Jensen, C. M. *J. Mater. Res.* **2005**, in press.
- (9) Gross, K. J.; Thomas, G. J.; Jensen, C. M. *J. Alloys Compd.* **2002**, 330–332, 683.
- (10) Kiyobayashi, T.; Srinivasan, S. S.; Sun D. and Jensen, C. M. *J. Phys. Chem. A* **2003**, 107, 7671.
- (11) Gross, K. J.; Guthrie, S.; Takara, S.; Thomas, G. *J. Alloys Compd.* **2000**, 297, 270.
- (12) Palumbo, O.; Cantelli, R.; Paolone, A.; Jensen, C. M. and Srinivasan, S. S. *J. Phys. Chem. B* **2005**, 109, 1168.
- (13) Brinks, H. W.; Jensen, C. M.; Srinivasan, S. S.; Hauback, B. C.; Blanchard, D.; Murphy, D. K. *J. Alloys Compd.* **2004**, 376, 215; Bastide, J. P.; Elhajri, J.; Claudy, P.; Elhajri, A. *Synth. React. Inorg. Metal-Organ. Chem.* **1995**, 25, 1037.
- (14) Huot, J.; Boily, S.; Guthrie, V.; Shultz, R. *J. Alloys Compd.* **1999**, 283, 304.
- (15) Zidan, R. A.; Takara, S.; Hee, A. G.; Jensen, C. M. *J. Alloys Compd.* **1999**, 285, 119.
- (16) Jensen, C. M.; Zidan, R. A. U.S. Patent 6,200,471,935.
- (17) Jensen, C. M.; Zidan, R. A.; Mariels, N.; Hee, A.; Hagen, C. *Int. J. Hydrogen Energy* **1999**, 24, 461.
- (18) Nowick, A. S.; Berry, B. S. *Anelastic Relaxation in Crystalline Solids*; Academic Press: New York, 1972.
- (19) Jensen, C. M.; Gross, K. *J. Appl. Phys. A* **2001**, 72, 213.
- (20) Wolverton, C.; Ozoliņš, V.; Asta, M. *Phys. Rev. B* **2004**, 69, 144109.
- (21) Fukai, Yuh and Okuma, N. *Phys. Rev. Lett.* **1995**, 73, 1640.
- (22) Cannelli, G.; Cantelli, R. In *Proceedings of the 6th International Conference on Internal Friction and Ultrasonic Attenuation in Solids*; Hasiguti, R. R., Mikoshiba, N., Eds.; University of Tokyo Press: 1977; p. 491.
- (23) Cannelli, G.; Cantelli, R.; Koiwa, M. *Philos. Mag. A* **1982**, 46, 483.
- (24) Cannelli, G.; Cantelli, R.; Cordero, F.; Trequattrini, F. In *Tunneling systems in amorphous and crystalline solids*; Esquinazi, P., Ed.; Springer-Verlag: Berlin, Heidelberg, 1998.
- (25) Cantelli, R.; Mazzolai, F. M.; Nuovo, M. *Phys. Stat. Sol.* **1969**, 34, 597.
- (26) Cannelli, G.; Cantelli, R. In *Proceedings of the 2nd International Conference on Hydrogen in Metals (Paris)*; Pergamon Press: Oxford, p. 395.
- (27) Iniguez, J.; Yildirim, T.; Udovic, T. J.; Sulic, M.; Jensen, C. M. *Phys. Rev. B* **2004**, 70, 60101.
- (28) Majzoub, E. H.; McCarty, K. F.; Ozoliņš, V. *Phys. Rev. B* **2005**, 71, 024118.
- (29) Rijssenbeek, J.; Gao, Y.; Srinivasan, S.; Jensen, C. M. manuscript in preparation.